Relativistic Newtonian dynamics

IOP Conf. Series: Journal of Physics: Conf. Series **845** (2017) 012028 doi:10.1088/1742-6596/845/1/012028

Relativistic Newtonian dynamics

Yaakov Friedman and Joseph Mendel Steiner

Jerusalem College of Technology
Departments of Mathematics and Physics
P.O.B. 16031 Jerusalem 9116001, Israel
email: friedman@jct.ac.il

E-mail: friedman@jct.ac.il

Abstract. A new Relativistic Newtonian Dynamics (RND) for motion under a conservative force capable to describe non-classical behavior in astronomy is proposed. The rotor experiments using Mössbauer spectroscopy with synchrotron radiation, described in the paper, indicate the influence of non-gravitational acceleration or potential energy on time. Similarly, the observed precession of Mercury and the periastron advance of binaries can be explained by the influence of gravitational potential energy on spacetime. The proposed RND incorporates the influence of potential energy on spacetime in Newton's dynamics. The effect of this influence on time intervals, space increments and velocities is described explicitly by the use of the concept of escape trajectory. For an attracting conservative static potential we derived the RND energy conservation and the dynamics equation for motion of objects with non-zero mass and for massless particles. These equations are subsequently simplified for motion under a central force. Without the need to curve spacetime, this model predicts accurately the four non-classical observations in astronomy used to test the General Relativity.

1. Introduction

Newton's laws of motion are still relevant today and continue to be used as an excellent approximation in everyday experience. At the end of the 19th century, most problems in physics could be addressed with classical Newton theory except:

- non-covariance of Maxwell equations under Galilean transformations
- Michelson-Morley experiment
- gravitational redshift
- the anomalous precession of Mercury's orbit

These indicate a logical incompleteness of Newtons laws of motion.

The first of these problems was resolved by Einstein with his theory of Special Relativity (SR), in which the observed rate of a moving clock differs from the rate of a stationary clock and depends on the clock's velocity. This implies that the Lorentz transformations are the correct spacetime transformations between inertial frames. Einstein's new velocity addition formula of SR also explained the Michelson-Morley experiment.

The gravitational redshift and the anomalous precession of Mercury's orbit, however, cannot be explained within the framework of SR. These problems were solved using Einstein's Theory of Gravitation commonly known as General Relativity (GR), in which he basically accounted

for gravity as an attribute of curved spacetime. As Princeton physicist Wheeler later described it: Spacetime tells matter how to move, matter tells spacetime how to curve.

Although Einstein's theories of relativity originate in the logical incompleteness of Newton's laws of motion, that incompleteness itself has not been understood completely, as yet, and therefore there are still global and chronic problems which still need further clarification. We propose that this incompleteness arises from the fact that *Newton's theory does not consider the influence of energy on spacetime.*

SR considers the influence of kinetic energy on spacetime. The curving of spacetime in GR can be regarded as an expression of the the influence of the gravitational potential on spacetime and the weak equivalence principle [29]. It is known [25] that the gravitational redshift (time dilation due to gravitational potential), can be derived solely from energy conservation and Planck's equation. But also for non-gravitational fields energy conservation and Planck's equation predict a time dilation depending on the position in space, However, none of the relativity theories considers the influence of *non-gravitational potential energy* on spacetime.

In our search for such an influence, we looked for the effect of (non-gravitational) acceleration on time. Our recent rotor experiments using Mössbauer spectroscopy and synchrotron radiation at PETRAIII, Hamburg and at ESRF, Grenoble indicate the existence of non-gravitational time dilation due to the acceleration.

All the above suggested to us to derive a new *Relativistic Newtonian Dynamics* (RND) defined as:

Definition 1. *RND is a dynamics incorporating the effects of any energy (gravitational or non-gravitational) on spacetime into classical Newtonian dynamics.*

We conjecture:

Conjecture 1. *RND provides the necessary relativistic corrections to Newtonian dynamics with the capability to explain all the above mentioned problems without the need for radical changes.*

Our derivation incorporates well established principles of relativity into Newtonian dynamics without any a priori assumptions.

Currently, RND incorporates the influence of potential energy on spacetime by invoking an extensions of Einstein's Equivalence Principle and the Clock Hypothesis (CH) to describe this influence. For an attracting conservative static potential with zero potential at infinity we derived the RND energy conservation and the dynamics equation for the motion of both objects with non-zero mass and for massless particles. The relativistic corrections of RND dynamics equation depend on the reduced potential $\hat{U}$- the potential per unit mass, and on $\nabla\hat{U}$ - the classical acceleration generated by this potential.

Specialising further these equations to a central inverse square force, predict accurately both the anomalous precession of Mercury [14] as well as the periastron advance of any binary [17], without the need of curving spacetime. RND predicts [16], [7] a chaotic behavior in the microscopic region similar to the probabilistic description in quantum mechanics.

In IARD2012 we presented [8] an Extended Relativistic Dynamics (ERD), based on the assumption that the CH is not valid (acceleration influences time in addition to the influence of the velocity of the comoving frame) which predicts [4] the existence of a maximal acceleration, explored in [5]. The relativistic correction of the dynamic equation in this model depends only on $\nabla\hat{U}$ the classical acceleration generated by this potential and on the value of the maximal acceleration. ERD predicts [10], [8] the discreteness of the radiation spectrum (compatible with Planck's Hypothesis for appearance of electromagnetic energy in quanta) for the harmonic oscillator in the microscopic region. However, ERD does not predicts correctly the astronomical observations mentioned above.

This suggests:

Conjecture 2. *The final RND model should incorporate the relativistic corrections from both RND and ERD to describe non-classical behavior in both astronomical and microscopic regions.*

2. Testing Einstein's Clock Hypothesis at PETRAIII

A cornerstone of Relativity Theory is the CH, stating that the rate of an accelerated clock is equal to that of a co-moving unaccelerated clock [3]. As it was shown [4] and [8], if the CH is false, (meaning that the rates of two clocks moving at different accelerations but with instantaneously equal velocities are different) then there exists a maximal acceleration a_m and an additional Doppler-type shift $\Delta f/f = a/a_m$ is predicted for an accelerated source of radiation [5] and [8].

The aim of the experiment performed in 2013 under the leadership of Ralf Rölsberger at the Dynamics Beamline P01 of the synchrotron PETRAIII at DESY, Hamburg, Germany was to test the CH by looking for this Doppler type shift between two sources with different acceleration. Time-domain interferometry based on nuclear resonant scattering was used to measure this shift.

Nuclear resonant absorption experiments with samples subject to high accelerations have been performed in the past to test special relativity via measurement of the transverse Doppler effect. The most prominent one is the experiment by Kündig, [22], who employed a resonant absorber mounted on a fast rotating disk. A reanalysis [20] of this experiment claimed a 20% deviation between the observed shift and the one predicted by SR. This deviation can be explained [4] by the failure of the CH and the existence of a maximal acceleration of $a_m = 10^{19} m/s^2$. However, since the current observation [15] revealed that non-random vibrations (not measured in the above experiment) also contribute to the shift, this estimate of a_m is questionable.

Since the expected shift is very small one must use tools very sensitive to such shift. Such an effect could be detected via the ^{57}Fe Mössbauer nuclear resonance that exhibits a relative linewidth of $\Gamma_0/E_0 = 3{*}10^{-13}$. High radial accelerations **a** were obtained with the rotors used in the magic-angle spinning technique of nuclear magnetic resonance (NMR). The rotor diameter was $d = 3mm$ with rotational frequencies of up to $15kHz$. The rotor is a hollow cylinder in which the Mössbauer foil was placed to cover its full inner circumference.

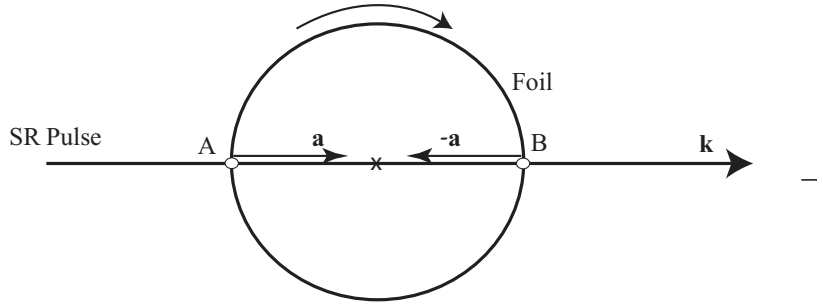

Figure 1. PETRAIII experimental geometry

The experimental geometry is shown in Figure 1. A focused beam of x-ray pulses (cross section $5 \times 5\mu m$ from the KB optics [19] at beamline P01, $1meV$ bandwidth) traversing the cylinder along its diameter perpendicular to its rotation axis meets the rotating ^{57}Fe foil twice: first, at the point of incidence A and then at the point of incidence B. The radial acceleration **a** is directed parallel at A and $-\mathbf{a}$ antiparallel at B to the photon wavevector **k**. Assuming that

acceleration causes a frequency shift, we expect a spectral shift between the resonant lines of the foil at the two points of incidence of the rotating cylinder. This spectral shift cannot be measured directly at this facility.

What could be measured at this facility is the so called *time spectrum*. A coherent pulse with frequency close to the resonant frequency of the sample, propagating through a sample, excites the nuclei in the sample thereby generating a delayed secondary radiation. The time spectrum of the sample is the intensity of this delayed radiation exiting the sample as a function of the delay time. In our case, the sample was the ^{57}Fe foil at the two points of incidence A and B. The formula for the time spectrum of a single resonant sample from a coherent synchrotron radiation pulse propagating through the sample obtained in [13] based on [1] is

$$I(\tau) \propto e^{-\tau} T^2 \left(\frac{J_1^2(\sqrt{T\tau})}{T\tau} + \alpha^2 J_0^2(\sqrt{T\tau}) \right), \tag{1}$$

where τ is the dimensionless time delay (the time delay divided by the lifetime of the excited level of the nuclei), T is the *effective thickness* of the sample, J_0, J_1 are the Bessel function of first kind of order zero and one, respectively and the constant $\alpha \ll 1$. In runs using an effectively thin foil, the only statistically significant parameter of the time spectrum is the effective thickness T. The measured effective thickness of the time spectrum of this rotating sample at different rotational frequencies is given in Figure 2.

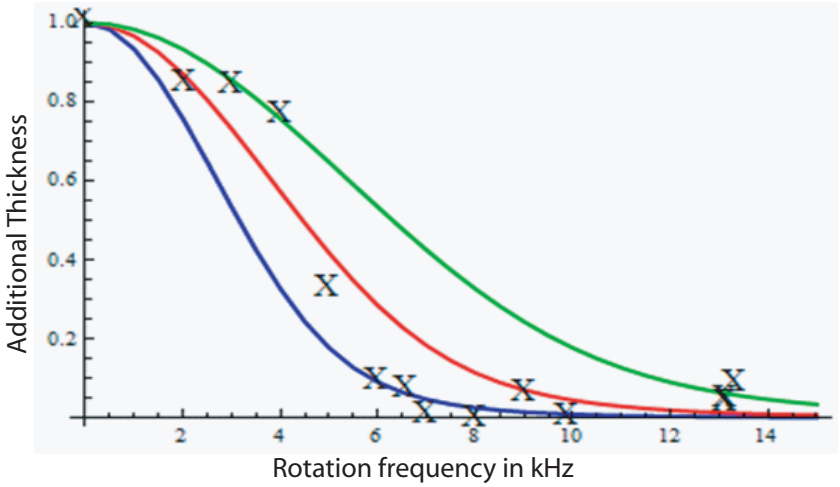

Figure 2. The measured × excess in the effective thickness of the time spectrum of the thin rotating sample at different rotational frequencies. Theoretical predictions for different values of a_m, Blue:$5 \cdot 10^{18}$, Red: 10^{19}, Green:$2 \cdot 10^{19} m/s^2$

The unit of thickness was chosen to be one for our foil and we reported the excess measured effective thickness relative to one foil. At rest, the measured effective thickness of the delayed radiation was twice the effective thickness of the foil (excess thickness one) because the radiation came from both points of incidence. The rotation of the sample will cause only a transverse Doppler shift of the sample spectrum, if the CH is valid, and this shift will be the same for both points of incidents. Such a shift does not affect the time spectrum, and one would not expect to get any effect on the time spectrum caused by rotation.

In the experiment we observed a gradual change from the spectrum at rest to the spectrum of one foil with the increase of the rotation frequency. Assuming that acceleration influences

time, this will cause a gradually increasing shift (similar to the usual Doppler shift) between resonant lines of the ^{57}Fe foil at the two points of incidence A and B. We observed that with rotations larger than 6kHz the effective thickness is the same as for one foil.

If there exists a strong shift between the absorption spectra at the two points of incidence at these rotational frequencies, as we expected, we may assume that their resonant frequencies are disjoint. Thus, the foil at B is transparent to the delayed radiation exiting A because of the difference in their resonant frequencies. Similarly, the radiation delayed at B was not delayed at A. Thus, the combined delayed radiation exiting the cylinder is a superposition of two rays, each of which was delayed only once. If the coherence between these two rays is lost, then the combined time spectrum will be that of a one foil spectrum. Thus, the results of the experiment indicate that the acceleration does effect time, contradicting the CH.

For an enriched sample the picture gets more complicated, indicating that probably there are additional unknown factors during the rotation affecting the time spectrum.

3. Testing acceleration time dilation at ESRF

Additional two experiments were performed at the European Synchrotron Radiation Facility (ESRF), Grenoble, France in 2014 and 2015. These experiments follow the outline presented in [8], see Figure 3. In [6] we predicted that the absorption line of a rotating Mössbauer absorber

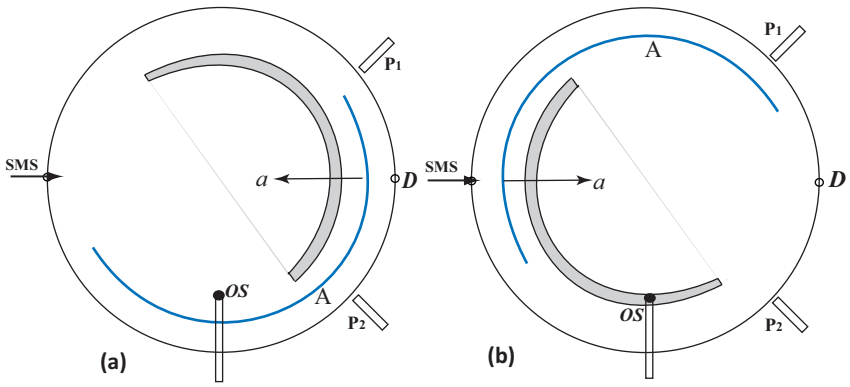

Figure 3. The setup and two states (a) and (b), SMS source, semicircular absorber A, optical sensor OS, proximity sensors P_1, P_2 and detector D

gets broader during the rotation. This is due to the fact that the beam must have a finite width. Therefore, the velocity of the absorber is not always perpendicular to all individual rays. Hence, these rays undergo a longitudinal Doppler shift in addition to the expected transversal one. This shift is very significant even for very narrow beams.

In 2014 experiment we confirmed experimentally [11] that, for a source outside the rotating disk, the absorption line of a rotating Mössbauer absorber is broadened during the rotation and that this broadening is linearly proportional to the rotation frequency. This necessitates the use of a strong Mössbauer source with the capability to focus the beam to the center of the disk. The Synchrotron Mössbauer Source (SMS) [26] at the Nuclear Resonance Beamline ID18 [27] of ESRF together with the KB-optics [19] to focus this beam, was the ideal choice for our experiments. The beam emitted by the SMS is almost fully resonant and fully polarized, has high brilliance and can be focused by use of KB-optics to a $10\mu m \times 5\mu m$ spot size at the center of the rotating disk. The beam from the SMS passes the KB-optics, hits the fast rotating semicircular absorber of radius $R = 0.05m$ and is finally detected by the APD detector D

diametrically opposed to the SMS (Figure 3). In this experiment we obtained for the first time the *entire resonant line* of a rotating absorber.

Based on the experiences of this experiment, a follow-up improved experiment was performed in 2015 at the same facility with the same rotor system. The main objective of this experiment was to explore the effect of acceleration on time dilation. The time dilation is measured by the shift in the Mössbauer resonant line of an accelerated absorber. The acceleration of the absorber was generated by rotating it using a rotor system. Using the setup diagrammatically presented in Figure 3 we separated the absorption of a rotating absorber into two states (a) and (b) when the acceleration is anti-parallel and parallel to the SMS radiation, respectively, and obtained the absorption lines for each state. Since the absorption line for each of the states are generated by the same source and absorber, and are equally affected by the velocity of the absorber with respect to the source, these two spectra should be identical without the influence of acceleration on time.

The experiment revealed [18] that within the given setup and rotation frequencies of 200Hz and higher, the resonant shifts of the two states are not the same. We observed a stable statistically significant non-zero relative shift between the spectral lines in the two states. In particular, for two long runs at 200 Hz in which the effect of vibrations was negligible, the almost constant relative shift of about $0.41(14) mm/s$, indicates the effect of acceleration on time dilation (see Figure 4 and Table 1). Existence of the statistically significant, almost

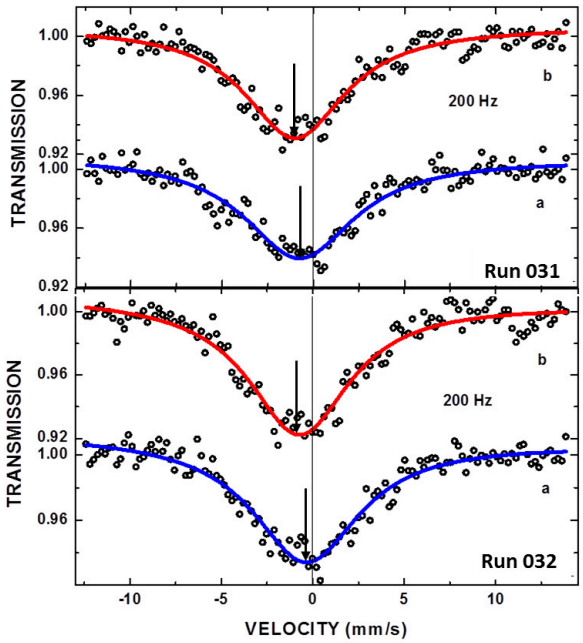

Figure 4. The absorption spectra, converted to average linear velocity form, of run 31 (top) and 32 (bottom) for states (a) and (b) at 200Hz rotation

constant, non-zero actual relative shift for two runs at 200 Hz indicates the effect of acceleration on the absorption resonant line and hence on time dilation.

Since non-gravitational accelerations were found to have an effect on time dilation, it would be interesting to compare this effect with that due to the redshift. To do this, one can imagine a massive object of mass M positioned at the center of the disk producing

Run	Effect %	γ [mm/s]	Shift x_0 [mm/s]	Vibr.sh.[mm/s]
31a	6.68(18)	3.29(24)	-0.58(11)	-0.007
31b	8.01(27)	3.14(22)	-1.01 (09)	0.007
32a	7.29(20)	3.25(20)	-0.22(12)	-0.01
32b	8.31(29)	3.13(21)	-0.61(09)	0.01

Table 1. Parameters of resonant spectra and the vibration shifts for states (a) and (b) at 200Hz rotation

a gravitational acceleration on the rim equal to centripetal acceleration in the experiment $a = R\omega^2 = 0.05(2\pi \cdot 200)^2 = 8 \cdot 10^4 m/s^2$. To achieve this acceleration on the rim $GM/R^2 = a$ requires that $GM = 197m^3/s^2$. The redshift in units of velocity due to such potential is $\frac{2GM}{Rc} = 0.013mm/s$. This value is more then one order of magnitude less then the observed relative shift. This is not surprising, since the rotation generate a non-conservative field, while gravitation is conservative. Moreover, since in both states the absorber is at the same gravitational potential level, one should not expect a relative redshift.

Currently, the only relativistic model that predicts a non-zero relative shift in such experiment is the ERD model [4],[5] which incorporates the influences of kinetic energy and acceleration assuming that Einstein's Clock Hypothesis is not valid and predicts a maximal acceleration. If we use the maximal acceleration $a_m = 10^{19} m/s^2$ based on Kündig's experiment [22] an an estimate, the observed relative shift is larger then expected. We plan to repeat the experiment with an improved system and study the dependence of the shift on frequency and direction of rotation.

A new RND theoretical model capable to explain the observed influence of the acceleration on time, as well as other phenomena in astronomy and microscopic region, is developed.

4. Relativistic Newtonian Dynamics

In this section we will derive the Relativistic Newtonian Dynamics (RND) for an attracting force with negative potential and apply it to astronomical predictions. This dynamics incorporates the influence of *any potential* energy vanishing at infinity into Newtonian dynamics. We begin by recalling some facts from Newtonian dynamics for a conservative force.

4.1. Newtonian dynamics under conservative force

We recall the description of the motion of a mass particle under a conservative force in Newtonian dynamics. Pick an inertial lab frame K with coordinates $\mathbf{x} = (x^1, x^2, x^3)$ and time t. We denote the mass of the particle by m, which will be assumed to be constant (rest mass), and denote the force by $\mathbf{F}(\mathbf{x})$ and its potential by $U(\mathbf{x})$. The trajectory $\mathbf{x}(t)$ of the motion of the particle is described by Newton's second law

$$m\frac{d^2\mathbf{x}(t)}{dt^2} = \mathbf{F}(\mathbf{x}(t)) = -\nabla U(\mathbf{x}(t)), \tag{2}$$

where ∇U denotes the gradient of U. Introduce a vector field $\mathbf{n}(\mathbf{x})$ which at any space point $\mathbf{x}$ is the normalized vector in the direction of the gradient $\nabla U(\mathbf{x})$, i.e.

$$\mathbf{n}(\mathbf{x}) = \nabla U(\mathbf{x})/|\nabla U(\mathbf{x})|. \tag{3}$$

Taking the dot product of this equation with $\mathbf{v} = d\mathbf{x}/dt$ we obtain

$$m\frac{d^2\mathbf{x}(t)}{dt^2} \cdot \frac{d\mathbf{x}}{dt} + \nabla U(\mathbf{x}) \cdot \frac{d\mathbf{x}}{dt} = \frac{d}{dt}\left(\frac{m}{2}\mathbf{v}^2 + U(\mathbf{x})\right) = 0$$

implying that the total energy E, which is a function of the state, defined by

$$E(\mathbf{x},\mathbf{v}) = \frac{m}{2}\mathbf{v}^2 + U(\mathbf{x}) \tag{4}$$

is conserved during the motion. The first term on the right-hand side is the kinetic energy and the second one is the potential energy.

From (2), the potential U is defined up to a constant. We will need a uniquely defined U satisfying the condition $U(\infty) = 0$. For an attractive force such U must be negative. Requiring the potential to vanish at infinity excludes polynomial potentials (e.g., oscillator) and other unbounded potentials and in its current status limits the applicability of the theory.

The *escape velocity* $v_e(\mathbf{x})$ is defined as the minimum speed in direction of $\mathbf{n}$ needed for a mass particle at $\mathbf{x}$ to "break free" from the attraction defined by the potential. More particularly, it is the velocity (speed traveled away from the starting point) at which the sum of a particle's kinetic and potential energies is equal to zero. Thus,

$$\boldsymbol{\beta}_e^2 := \frac{v_e^2(\mathbf{x})}{c^2} = -\frac{2U(\mathbf{x})}{mc^2}. \tag{5}$$

We further define the *Schwarzschild region*, the region S defined by

$$S = \{\mathbf{x} : \ \boldsymbol{\beta}_e^2(\mathbf{x}) \leq 1\}. \tag{6}$$

Any mass particle positioned in S cannot escape the attraction of the potential and will be absorbed. We will consider only motion outside S.

4.2. Influence of the potential energy on time intervals, space increments and velocity
Let $U(\mathbf{x})$ be the gravitational potential of an attracting static force field at any space point $\mathbf{x}$ in an inertial lab frame K. We assume that $U(\mathbf{x})$ is zero at infinity, where the attraction tends to zero. We will describe the *influence of the potential energy* $U(\mathbf{x})$ on spacetime in the neighbourhood of any space point $\mathbf{x}_0$.

Define the *escape trajectory* $\mathbf{x}(\tau)$ for some parameter τ as the (de)accelerated trajectory of the test object with velocity $\mathbf{v}_e(\mathbf{x}_0)$ defined by (5) at $\mathbf{x}_0$ and progressing freely to the ultimate point O with zero potential. Denote by $\tilde{K}(\mathbf{x}(\tau))$ the Frenet frames [12] defined by this escape trajectory, by K' the comoving frame to the accelerated frame $\tilde{K}(\mathbf{x}_0)$, and by $\tilde{K}(O)$ the final frame on this trajectory. Note that since $\tilde{K}(O)$ is an inertial frame in which the potential is time independent, it can be viewed as a translation of the lab frame K. Since the time intervals and space increments are not affected by a translation, the increments in $\tilde{K}(O)$ are the same as in the lab frame K.

On the escape trajectory the total energy E is zero, implying the equality of the kinetic and potential energies on this trajectory. Moreover, since there is a continual exchange between these two energies, it is natural to postulate a conjecture similar to the Equivalence Principle:

Conjecture 3. *The influence of the potential energy on spacetime in the neighbourhood of* $\mathbf{x}_0$ *is the same as the influence of the acceleration and velocity on rest points in the accelerated frame* $\tilde{K}(\mathbf{x}(\tau))$ *defined by the escape trajectory at* $\mathbf{x}_0$.

This conjecture allows one to express the effect of the potential energy on the time intervals and space increments, by their corresponding changes from $\tilde{K}(\mathbf{x}_0)$ to $\tilde{K}(O)$. Then, using an extension of Einstein's CH, introduced in [9, 12] and [23, 24], one can quantify these changes by the use of the Lorentz spacetime transformation between the frames K'-the comoving frame to $\tilde{K}(\mathbf{x}_0)$ and $\tilde{K}(O)$. Finally, since since increments in $\tilde{K}(O)$ are the same as in K, one can express

the effect of the potential energy on the time and space increments by a map $\Phi : \tilde{K}(\mathbf{x}_0) \to K$ based on the Lorentz transformation from K' to K. Using (5) this map is

$$\Phi(dt) = \tilde{\gamma}dt,\ \Phi(d\mathbf{x}_n) = \tilde{\gamma}d\mathbf{x}_n,\ \Phi(d\mathbf{x}_{tr}) = d\mathbf{x}_{tr}\,, \tag{7}$$

where

$$\tilde{\gamma} = \frac{1}{\sqrt{1 - v_e^2(\mathbf{x}_0)/c^2}} = \frac{1}{\sqrt{1 + 2U(\mathbf{x}_0)/mc^2}} \tag{8}$$

and the components of the space increments in the direction $\mathbf{n}$ and transverse to $\mathbf{n}$ are

$$d\mathbf{x}_n = (d\mathbf{x} \circ \mathbf{n})\mathbf{n},\ \ d\mathbf{x}_{tr} = d\mathbf{x} - (d\mathbf{x} \circ \mathbf{n})\mathbf{n} \tag{9}$$

with $\circ$ denoting the Euclidean dot product and $\mathbf{n}$ defined by (3) is the direction of the escape velocity.

Note that $\tilde{\gamma}$ defined by (8) is the known gravitational *time dilation factor*, if $U(\mathbf{x})$ represents a gravitational potential. From (7) it follow that the influence of potential energy at $\mathbf{x}_0$ on any 3D velocity $\mathbf{v} = \frac{d\mathbf{x}}{dt}$, expressed by the map Φ, is

$$\Phi(\mathbf{v}_n) = \mathbf{v}_n,\ \Phi(\mathbf{v}_{tr}) = \tilde{\gamma}^{-1}\mathbf{v}_{tr}. \tag{10}$$

This means, that the velocity of an object at $\mathbf{x}_0$ is spacetime influenced by the potential energy is transformed to the velocity in the lab frame K by multiplying the component of the velocity transverse to $\mathbf{n}$ by $\tilde{\gamma}^{-1}$, where the time dilation factor $\tilde{\gamma}$ is defined by (8).

4.3. RND energy conservation

As shown above, the potential energy influences time intervals and space increments in the direction of $\mathbf{n}(\mathbf{x})$, while the space increments transverse to $\mathbf{n}(\mathbf{x})$ are not influenced by this potential energy. We obtain the RND energy conservation formula, by analogy to the principle of least action, a variational principle that defines the path of motion as the path with the least value of some action. In an analogous way the motion in such an influenced spacetime can be viewed as the motion along a geodesic (path with least distance) with respect to some metric. By the above observation this metric is of the form

$$ds^2 = f(\mathbf{x})(cdt)^2 - g(\mathbf{x})d\mathbf{x}_n^2 - d\mathbf{x}_{tr}^2, \tag{11}$$

where the two vector projections of the space increments $d\mathbf{x}_n$ and $d\mathbf{x}_{tr}$ parallel and transverse to $\mathbf{n}(\mathbf{x})$ are defined by (9) and the positive valued functions $f(\mathbf{x}), g(\mathbf{x})$ describe the influence of the potential energy on the time intervals and space increments in the $\mathbf{n}(\mathbf{x})$ direction.

Consider now the time dilation due to the influence of potential energy of a clock resting at some point $\mathbf{x}$ in K. Since for such a clock $d\mathbf{x} = 0$, from (11) $ds = \sqrt{f(\mathbf{x})}cdt$ implying that the time dilation of such a clock is $c\frac{dt}{ds} = \frac{1}{\sqrt{f(\mathbf{x})}}$. From (7), this time dilation is defined by the gamma-factor $\tilde{\gamma}$ given by (8), implying that $\sqrt{f(\mathbf{x})} = \sqrt{1 + 2U(\mathbf{x})/mc^2}$. Introducing the *dimensionless potential energy*

$$u(\mathbf{x}) = \frac{-2U(\mathbf{x})}{mc^2}, \tag{12}$$

one obtains immediately

$$f(\mathbf{x}) = 1 - u(\mathbf{x}). \tag{13}$$

This formula reduces to the gravitational time dilation in the vicinity of a non-rotating massive spherically symmetric object, as derived from the Schwarzschild metric.

The motion of an object of mass $m > 0$ along a time-like geodesic $\mathbf{X}(\lambda) = (ct(\lambda), \mathbf{x}(\lambda))$ in spacetime is parameterized by an *affine parameter* λ on the trajectory, chosen to be the arc length s defined by (11). For massless objects (photons) moving along light-like geodesics $ds = 0$, this affine parameter is redefined as in [25] p.575 with the normalization condition

$$\lim_{x^2 \to \infty} c\frac{dt}{d\lambda} = 1. \tag{14}$$

The four-velocity on the trajectory is $\dot{\mathbf{X}} = \frac{d\mathbf{X}}{d\lambda} = (c\dot{t}, \dot{\mathbf{x}})$, where *dot* denotes differentiation with respect to λ.

Since the metric (11) is independent of t, the vector $\mathbf{K}_0 = (1, 0, 0, 0)$ is a Killing vector ([25], p.651) and its scalar product $\dot{\mathbf{X}} \cdot \mathbf{K}_0$ with respect to this metric with the four-velocity is conserved on the trajectory. Thus, on any trajectory there exists a constant k related to the total energy on it such that

$$cf(\mathbf{x})\dot{t} = k, \quad c\dot{t} = \frac{k}{1 - u(\mathbf{x})}. \tag{15}$$

Using (11),(13) and (15), the four-velocity norm is

$$\dot{\mathbf{X}}^2 = \frac{k^2}{1 - u(\mathbf{x})} - g(\mathbf{x})\dot{\mathbf{x}}_n^2 - \dot{\mathbf{x}}_{tr}^2 = \epsilon, \tag{16}$$

where $\epsilon = 1$ for objects with non-zero mass and $\epsilon = 0$ for massless particles. For objects with non-zero mass multiply this equation by $(1 - u(\mathbf{x}))$ to obtain

$$(1 - u(\mathbf{x}))g(\mathbf{x})\dot{\mathbf{x}}_n^2 + (1 - u(\mathbf{x}))\dot{\mathbf{x}}_{tr}^2 - u(\mathbf{x}) = k^2 - 1\,. \tag{17}$$

This formula can be considered as the RND dimensionless energy conservation equation on the trajectory. The first two terms of the left side are the relativistically corrected dimensionless kinetic energy (the square of the influenced dimensionless velocity $\Phi(\dot{\mathbf{x}})^2$) and the third term is the dimensionless potential energy. The right side is the dimensionless total energy $k^2 - 1$.

To calculate the influenced dimensionless kinetic energy, note that $\dot{\mathbf{x}} = \dot{t}\mathbf{v}$, where $\mathbf{v} = \frac{d\mathbf{x}}{dt}$ and using (10) and that $\tilde{\gamma}^{-2} = 1 - u$ one obtains

$$\Phi(\dot{\mathbf{x}})^2 = \dot{t}^2\Phi(\mathbf{v})^2 = \dot{t}^2(\mathbf{v}_n^2 + (1 - u(\mathbf{x}))\mathbf{v}_{tr}^2) = \dot{\mathbf{x}}_n^2 + (1 - u(\mathbf{x}))\dot{\mathbf{x}}_{tr}^2.$$

Comparing this to the first two terms in (17) one obtains

$$g(\mathbf{x}) = \frac{1}{1 - u(\mathbf{x})}, \tag{18}$$

hence, the RND dimensionless energy conservation equation for an object with non-zero mass becomes

$$\dot{\mathbf{x}}_n^2 + (1 - u(\mathbf{x}))\dot{\mathbf{x}}_{tr}^2 - u(\mathbf{x}) = \mathcal{E}, \tag{19}$$

where the dimensionless total energy on the trajectory is $\mathcal{E} = 2E/mc^2 = k^2 - 1$.

For a massless particle, the analysis is only applicable when restricted to a gravitational potential for which the dimensionless potential energy $u(\mathbf{x})$ is independent of the mass m. For such a potential one can define a *reduced potential* or potential per unit mass as

$$\hat{U} = \frac{U}{m}. \tag{20}$$

For such potential, the dimensionless potential defined by (12) is $u(\mathbf{x}) = -2\hat{U}/c^2$. For such particle ($\epsilon = 0$), multiplying (16) by $(1 - u(\mathbf{x}))$ and using (18) one obtains

$$\dot{\mathbf{x}}_n^2 + (1 - u(\mathbf{x}))\dot{\mathbf{x}}_{tr}^2 = k^2. \tag{21}$$

Even though gravitation does not act directly on the photon as a force since its mass is zero, which is expressed in missing term $-u(\mathbf{x})$ in (19), its momentum and angular momentum are not zero and its motion is affected by the influence of the gravitational potential on spacetime expressed by the relativistic term in this equation. Moreover, from (14) and (15) one obtains $k = 1$.

Thus, the RND dimensionless energy conservation equation for both objects with non-zero mass and massless particles is

$$\dot{\mathbf{x}}_n^2 + (1 - u(\mathbf{x}))\dot{\mathbf{x}}_{tr}^2 - \epsilon u(\mathbf{x}) = 1 + \epsilon(\mathcal{E} - 1). \tag{22}$$

Unlike in GR, in RND the reduced energy (obtained by multiplying the dimensionless energy by $c^2/2$)

$$H(\mathbf{x}, \dot{\mathbf{x}}) = \frac{c^2\dot{\mathbf{x}}^2}{2} + \hat{U}(\mathbf{x})(\dot{\mathbf{x}}^2 - (\dot{\mathbf{x}} \circ \mathbf{n})^2) + \epsilon\hat{U}(\mathbf{x}) \tag{23}$$

is conserved on the trajectory. Note that the relativistic addition to a classical reduced total energy, expressed in the middle term of right-hand side, depends both on the potential energy at that point and the velocity of the moving object.

4.4. RND Equation of Motion under a Conservative Force

By use of (9) equation (22) can be rewritten as

$$\dot{\mathbf{x}}^2 - \epsilon u(\mathbf{x}) - u(\mathbf{x})(\dot{\mathbf{x}}^2 - (\dot{\mathbf{x}} \circ \mathbf{n})^2) = 1 + \epsilon(\mathcal{E} - 1). \tag{24}$$

The equation of motion is obtained by differentiating (24) by λ which leads to

$$2\ddot{\mathbf{x}} \circ \dot{\mathbf{x}} - \epsilon\dot{u} - \dot{u}\dot{\mathbf{x}}_{tr}^2 - 2u(\ddot{\mathbf{x}} \circ \dot{\mathbf{x}} - (\dot{\mathbf{x}} \circ \mathbf{n})(\ddot{\mathbf{x}} \circ \mathbf{n} + \dot{\mathbf{x}} \circ \dot{\mathbf{n}})) = 0,$$

Substituting $u(\mathbf{x}) = -\hat{2}U/c^2$ and its derivative $\dot{u} = -\frac{2\nabla\hat{U} \circ \dot{\mathbf{x}}}{c^2}$, one obtains

$$\ddot{\mathbf{x}} + \frac{2\hat{U}(\mathbf{x})}{c^2}\ddot{\mathbf{x}}_{tr} = -\frac{\epsilon\nabla\hat{U}}{c^2} - \frac{\nabla\hat{U}\dot{\mathbf{x}}_{tr}^2}{c^2} + \frac{2\hat{U}}{c^2}(\dot{\mathbf{x}} \circ \dot{\mathbf{n}})\mathbf{n}. \tag{25}$$

Decomposing this vector equation into the parallel and perpendicular components to $\mathbf{n}$, the perpendicular component is

$$\left(1 + \frac{2U(\mathbf{x})}{mc^2}\right)\ddot{\mathbf{x}}_{tr} = 0. \tag{26}$$

implying that $\ddot{\mathbf{x}}_{tr} = 0$ for $\mathbf{x}$ outside the Schwarzschild region defined by(6).

Thus, for motion outside the Schwarzschild region the *RND equation of motion* for any object/particle is

$$c^2\ddot{\mathbf{x}} = -\epsilon\nabla\hat{U} - \dot{\mathbf{x}}_{tr}^2\nabla\hat{U} + 2\hat{U}(\mathbf{x})(\dot{\mathbf{x}} \circ \dot{\mathbf{n}})\mathbf{n}. \tag{27}$$

Noting that $\frac{d}{d\lambda} = \frac{k}{c(1-u)}\frac{d}{dt}$ from (15) and remembering that $\mathbf{v} = \frac{d\mathbf{x}}{dt}$ one obtains the RND equation of motion in the space and time of the lab frame K as

$$\frac{k^2}{1-u}\frac{d}{dt}\left(\frac{\mathbf{v}}{1-u}\right) = -\epsilon\nabla\hat{U} - \frac{k^2\mathbf{v}_{tr}^2\nabla\hat{U}}{c^2(1-u)^2} + \frac{2k^2\hat{U}}{c^2(1-u)^2}(\mathbf{v} \circ \frac{d\mathbf{n}}{dt})\mathbf{n}. \tag{28}$$

Note that the acceleration $\frac{d^2\mathbf{x}}{dt^2}$ is not in the direction of $\mathbf{n}$, but $\ddot{\mathbf{x}}$ is.

The first relativistic correction depends on $-\nabla\hat{U}$- the classical acceleration caused by the force, and the second one depends on the reduced potential $\hat{U}$. Unlike in the classical Newtonian equation of motion involving only the force $\mathbf{F}$, the RND equation involves both the potential U (as in Schrodinger quantum dynamics equation) as well as ∇U.

4.5. Central force motion in RND

Let $U(r)$ be a potential of a central force which is attractive and static in an inertial lab frame K with origin at the center of the force. Assume that $U(r)$ is negative and vanishes at infinity. In this case $\mathbf{n}$ defined by (3) is the radial direction and from (7) it follows that the time intervals and the radial spacial displacements are influenced by the potential energy, while the spacial displacements transverse to the radial direction are not affected.

Introduce spherical coordinates r, φ, θ in K. Using the results of Section 4.3, the influence of the potential energy on spacetime in the neighbourhood of any point is described by the metric

$$ds^2 = (1-u(r))(cdt)^2 - \frac{1}{1-u(r)}(dr)^2 - r^2((d\theta)^2 + \sin^2\theta(d\varphi)^2). \tag{29}$$

As above, assume that the motion of an object/particle is along the geodesic in spacetime $\mathbf{X}(\lambda) = (t(\lambda), r(\lambda), \varphi(\lambda), \theta(\lambda))$ parameterised by the affine parameter λ. Then the four-velocity is $\dot{\mathbf{X}} = \frac{d\mathbf{X}}{d\lambda} = (c\dot{t}, \dot{r}, \dot{\varphi}, \dot{\theta})$. From symmetry considerations one may assume that if initially the position and velocity of the object/particle are in the plane $\theta = \pi/2$, they will remain in this plane during the motion. Thus, one may assume that $\theta = \pi/2$ and $\dot{\theta} = 0$.

Using that the metric is independent of φ, the vector $\mathbf{K}_3 = (0, 0, 1, 0)$ is a Killing vector implying that

$$J = r^2\dot{\varphi} \tag{30}$$

remains constant on the trajectory, where cJ has the meaning of angular momentum per unit mass for objects with non-zero mass and J has units of length.

Using that $\dot{\mathbf{x}}_n = \dot{r}$ and that $\dot{\mathbf{x}}_{tr}^2 = \frac{J^2}{r^2}$ one can rewrite the RND dimensionless energy conservation equation (22) as

$$\dot{r}^2 + (1-u(r))\frac{J^2}{r^2} - \epsilon u(r) = 1 + \epsilon(\mathcal{E} - 1). \tag{31}$$

Using (30) and (31) one obtains the parameter-free equation for the trajectory $r(\varphi)$

$$\left(\frac{J}{r^2}\frac{dr}{d\varphi}\right)^2 + (1-u(r))\frac{J^2}{r^2} - \epsilon u(r) = 1 + \epsilon(\mathcal{E} - 1). \tag{32}$$

This equation with $\epsilon = 1$ was used in the previous papers [14], [16] and [17] for objects with non-zero mass.

Introducing polar coordinates and complex numbers in the plane $\theta = \pi/2$, $\mathbf{r} = re^{i\varphi}$. Using (30),

$$\dot{\mathbf{r}} = \dot{r}e^{i\varphi} + ri\dot{\varphi}e^{i\varphi} = \dot{r}e^{i\varphi} + i\frac{J}{r}e^{i\varphi}. \tag{33}$$

and

$$\ddot{\mathbf{r}} = \ddot{r}e^{i\varphi} + \dot{r}\frac{J}{r^2}ie^{i\varphi} - \dot{r}\frac{J}{r^2}ie^{i\varphi} - \frac{J^2}{r^3}e^{i\varphi} = \left(\ddot{r} - \frac{J^2}{r^3}\right)e^{i\varphi}.$$

For a central force $\mathbf{n} = e^{i\varphi}$ and using (33) and (30), $\dot{\mathbf{r}} \cdot \dot{\mathbf{n}} = \frac{J^2}{r^3}$. Substituting this into (27), the *RND equation of motion for a central force* becomes

$$c^2\left(\ddot{r} - \frac{J^2}{r^3}\right) = -\epsilon\nabla\hat{U} - \frac{J^2}{r^2}\nabla\hat{U} + \frac{2\hat{U}(\mathbf{r})J^2}{r^3}. \tag{34}$$

This equation defines $r(\lambda)$. Then, equation (30) defines $\varphi(\lambda)$ and hence the trajectory of any object/particle.

4.6. Inverse square law in RND
Consider now a inverse square law force $\mathbf{F}(\mathbf{r})/m = -\frac{w}{r^3}\mathbf{r}$ with potential $\hat{U}(\mathbf{r}) = -\frac{w}{r}$. Substituting this into (34) one obtains

$$\left(\ddot{r} - \frac{J^2}{r^3}\right) = -\frac{w}{c^2 r^2} - \frac{wJ^2}{c^2 r^4} - \frac{2wJ^2}{c^2 r^4},$$

or

$$\ddot{r} = \frac{J^2}{r^3} - \frac{w}{c^2 r^2} - \frac{3J^2 w}{c^2 r^4}. \tag{35}$$

Note that for this case the two relativistic correction reinforce each other.

This equation is further simplified if one expresses it in terms of $u(\varphi)$ defined by (8) as $u(r) = \frac{2w}{c^2 r} = \frac{r_s}{r}$ with $r_s = \frac{2w}{c^2}$. Denoting by $u' = \frac{du}{d\varphi}$ it can be shown by use of (30) that $\dot{r} = -\frac{J}{r_s}u'$ and $\ddot{r} = -\frac{J^2}{r_s r^2}u''$. With these substitutions (35) becomes

$$-\frac{J^2}{r_s^3}u^2 u'' = \frac{J^2}{r_s^3}u^3 - \frac{w}{r_s^2}u^2 - \frac{3J^2 w}{c^2 r_s^4}u^4, \tag{36}$$

which simplifies to

$$u'' + u = \frac{r_s w}{J^2} + \frac{3w}{c^2 r_s}u^2.$$

Using the definition of r_s one obtains

$$u'' + u = \frac{2w^2}{c^2 J^2} + \frac{3}{2}u^2. \tag{37}$$

The relativistic correction turns the linear classical Newtonian equation into a non-linear one.

Defining the orbit parameter $\mu = \frac{2w^2}{c^2 J^2}$, equation (37) reproduces equation (25) in [14] for planetary motion under RND which predicts the known anomalous precession $3\pi\mu$ of Mercury [2], [21]. Note that the first relativistic correction term of (34) depending on the force contributes $\pi\mu$ to the precession, while the second correction term depending on the potential contributes $2\pi\mu$ to the precession.

Furthermore, the two body problem has also a solution in RND. Using a similar analysis as above, we have shown in [17] that RND is able to handle effectively the periastron advance of any binary. For a hydrogen-like atom RND predicts [16] a chaotic behavior compatible to the probabilistic model of quantum mechanics.

The RND model also handles motion with unbounded trajectories, predicts accurately gravitational lensing and the Shapiro time delay for a light ray passing in vicinity of a spherically symmetric massive object. These will appear in future publications.

5. Discussion and conclusions

The observed anomalous precession of Mercury and periastron advance of the Hulse-Taylor pulsar and other binaries were predicted by the authors [14], [17] by considering the influence of potential energy on spacetime. Our recent experiments [18] indicate that non-gravitational acceleration also influences time. Suchard [28] also predicts that the potential of an electromagnetic field influences spacetime. These suggest that any potential energy, gravitational or not, influences spacetime.

In order to understand how the laws of dynamics should be modified by this influence, one must express explicitly the relativistic corrections due to it. A new RND model is proposed to describe non-classical behavior. So far we have shown that this model passes successfully all the

non-classical tests in astronomy used for the justification of GR. But this model is not limited to gravitation and could be applied to other conservative fields, like the electric field. So, it has a potential to describe the non-classical behavior of the microscopic world.

In Sections 2 and 3, we presented our recent experiments using Mössbauer spectroscopy of a rotating absorber and synchrotron radiation which indicate the influence of non-gravitational acceleration on time.

The RND was then derived in Section 4 for a conservative static attracting force with zero potential at infinity. The influence of the potential energy on spacetime in the neighbourhood of a point $\mathbf{x}_0$ is described by the use of the escape trajectory and conjecturing that this influence is the same as the influence of velocity and acceleration on the escape trajectory initiating at this point. Then, this influence can be described by the transformation from the the initial accelerated frame at $\mathbf{x}_0$ to the final inertial (lab) frame on the escape trajectory. The transformation in the model is bases on the validity of the CH for an accelerated system in flat spacetime.

The RND reduced total energy (23) for objects of non-zero mass and massless particles introduce an additional term depending on both the kinetic and potential energies into the classical energy equation (4). The RND equation of motion (27) introduce two relativistic correction terms of order 2 in v/c into. The first relativistic correction depends on $-\nabla\hat{U}$- the classical acceleration caused by the force, and the second one depends on the reduced potential $\hat{U}$- potential per unit mass.

For a central force, using angular momentum conservation (30), the RND equation of motion is simplified (34) and even more for an inverse square law (35) leading to a single additional relativistic term to the classical equation. This equation predicts accurately the anomalous precession of Mercury and periastron advance of any binary. These deviations from Newtonian behavior in these astronomical observations were predicted by GR and experimentally confirm its validity for weak gravitational fields only [29]. Recently we have shown that RND predicts accurately gravitational lensing and Shapiro time delay of light as it moves over a finite distance through a change in the gravitational potential of a massive spherically symmetric object M. Thus, RND passes successfully all four tests of GR.

As mentioned above, one of the limitations of the current RND model is the requirement of zero potential at infinity - zero point of the force. Even though the force generated by the harmonic oscillator is conservative and its potential could be defined to be zero at the point where the force is zero, this zero point is not at infinity and an escape trajectory cannot be defined properly in this model. So, it is not surprising that when the RND dynamics equation of motion is applied to the oscillator, the relativistic correction terms cancel out. So RND in its current form is not able to describe the change of behavior of the oscillator in the microscopic region involving strong fields. The needed modifications for strong fields can be obtained by use of Extended Relativistic Dynamics (ERD) [5]. In ERD the speed of any moving object is limited by c and the magnitude of its acceleration is limited by a_m. The relativistic correction in ERD depends only on the classical acceleration caused by the force $-\nabla\hat{U}$. It was shown [10] that the vibrations of the ERD harmonic oscillator poses an identical spectrum to that of the quantum oscillator in the microscopic region, which implies Planck's assumption.

We plan to extend RND also for non-conservative forces by use of a four-potential instead of the scalar potential. We plan to study the implications of this model to the electromagnetic field and experimentally test these implications.

In order to predict accurately both astronomical observations and the dynamics in the microscopic region, both RND and ERD corrections together with an extension of the model to non-conservative forces is probably needed.

References

[1] Burnham D C and Chiao R Y *Phys. Rev.* **188** (1969) 667-675

[2] Grøn Ø, Hervik S. 2007 *Einstein's General Theory of Relativity: With Modern Applications in Cosmology* (Springer)
[3] Einstein A 1907 *Jahrb. Radioakt. Elektron.* **4** 411
[4] Friedman Y, Gofman Yu 2010 *Phys. Scr.* **82** 015004
[5] Friedman Y 2011 *Ann. Phys. (Berlin)*, **523 523** 408-416.
[6] Friedman Y, Nowik I 2012 *Phys. Scr.* **85** 065702
[7] Friedman Y, Resin E 2012 *Phys. Scr.* **86** 015002
[8] Friedman Y 2013 *Proc. of IARD 2012, J. of Phys.: Conf. Ser.* **437** 012017
[9] Friedman Y, Scarr T 2013 *Phys. Scr.* **87** 055004
[10] Friedman Y 2013 *Phys. Scr.* **87** 065702
[11] Friedman Y *et al.* 2015 *J. Synch. Rad.* **22** 723
[12] Friedman Y, Scarr T 2015 *Gen. Relat. and Grav.* **47** 121
[13] Friedman Y, Steiner J M, Yudkin E 2015 *Eur. Phys. Lett.* **111** 34003
[14] Friedman Y, Steiner J M 2016 *Eur. Phys. Lett.***113** 39001
[15] Friedman Y *et al.* 2016 *Eur. Phys. Lett.* **114** 50010
[16] Friedman Y 2016 *Eur. Phys. Lett.* **116** 19001
[17] Friedman Y, Livshitz S, Steiner J M 2016 *European Physics Letters* **116** 59001
[18] Friedman Y *et al.* 2017 *Advances in testing the effect of acceleration on time dilation using a Synchrotron Mössbauer Source*, *J. Synch. Rad.*, to appear
[19] Kirkpatrick P, Baez A V 1948 *J. Opt. Soc. Am.* **38** 766
[20] Kholmetskii A L, Yarman T and Missevitch O V, 2008 *Phys. Scr.* **77** 035302
[21] Kopeikin S, Efroimsky M, Kaplan G 2011 *Relativistic Celestial Mechanics of the Solar System* (Wiley-VCH, Berlin)
[22] Kündig W 1963 *Phys. Rev.* **126** 2371
[23] Mashhoon B 1990 *Phys. Lett. A* **143** 176-182
[24] Mashhoon B 1990 *Phys. Lett. A* **145** 147-153
[25] Misner C W, Thorne K S and Wheeler J A *Gravitation* Freeman and co.(1973)
[26] Potapkin V, Chumakov A I, Smirnov G V, Celse J-P, Rüffer R, McCammon C and Dubrovinsky L 2012 *J. Synch. Rad.* **19** 559
[27] Rüffer R,Chumakov A I 1996 *Hyp. Int.*, **97/98** 589-604
[28] Suchard E H 2015 *Physical Science International Journal* **7** 152
[29] Will C M 2014 *Liv. Rev. Relat.* **17** 4